Analytical Study of the Seismic Behaviour of Beam-Column Elements Reinforced with Superelastic Shape Memory Alloy

M.S. Alam[1], M.A. Youssef[2] and M. Nehdi[3]

[1]Ph.D. Candidate, Dept of Civil and Environmental Engineering, the University of Western Ontario, London, ON, N6A5B9, Canada, malam8@uwo.ca

[2]Assistant Professor, Dept of Civil and Environmental Engineering, the University of Western Ontario, London, ON, N6A5B9, Canada, youssef@uwo.ca

[3]Associate Professor, Dept of Civil and Environmental Engineering, the University of Western Ontario, London, ON, N6A5B9, Canada, mnehdi@eng.uwo.ca

Abstract

Recently two experimental investigations were carried out on beam-column elements under seismic loading, one in the University of Western Ontario and the other in the University of Nevada, Reno, where superelastic Shape Memory Alloy (SMA) rebars were used as reinforcement at their plastic hinge regions. Such SMA reinforced beam-column elements experienced reduced residual deformation at the end of seismic loading. This study aims in developing finite element (FE) models in order to simulate the seismic behaviour of SMA-reinforced concrete (RC) beam-column elements. The predicted behaviour of the two specimens from FE analysis, their load-storey drift relationship, and energy dissipation ability are compared with the experimental results. The results showed that the model could predict the behaviour of both SMA-RC beam-column elements with reasonable accuracy.

Keywords: finite element model, beam-column element, seismic, shape memory alloy, superelasticity.

Introduction

Large-scale earthquake events cause severe damage to infrastructure resulting in collapses of buildings, closing of bridges, unattainable post-disaster rescue operations, and overall substantial economic losses. These can generally be avoided if structures were serviceable after such earthquakes. Superelastic (SE) Shape Memory Alloy (SMA) is a special material that can undergo large inelastic deformations and recover its original shape by stress removal, thus mitigating the problem of permanent deformation. Because of its unique characteristics, SMAs have gained increased usage in structural applications[1] for instance, as column anchorage[2], frame

bracing[3], concrete prestressing[4], damping device[5], and bridge restrainers[6]. Recent tests conducted by Wang[7] and Youssef et al.[8] showed that SE SMA RC elements are capable of dissipating significant amounts of energy with negligible residual deformation and rotation during earthquakes. This extraordinary characteristic of SE SMA-RC beam-column elements can have a great benefit in highly seismic areas, where such RC members can remain functional even after a strong earthquake. Their high strength, large energy hysteretic behaviour, full recovery of strains up to 8%, high resistance to corrosion and fatigue make them strong contenders for use in earthquake resistant structures[9]. In particular, Ni-Ti alloy has been found to be the most promising SMA for seismic applications.

This paper reviews the fundamental characteristics and the modeling technique of SE SMA. Nonlinear FE analysis has been implemented in this study to predict the load-displacement relationship and energy dissipation capacity of superelastic SMA RC beam-column elements and compare it to the experimental results.

Superelastic Shape Memory Alloy and its Modelling

Superelasticity is a distinct property that makes SMA a smart material. A SE SMA can restore its initial shape spontaneously even from its inelastic range upon unloading. Among various composites, Ni-Ti has been found to be the most appropriate SMA for structural applications because of its large recoverable strain, superelasticity and exceptionally good resistance to corrosion. In this paper, unless otherwise stated, SMAs are mainly referred to Ni-Ti SMA (commonly known as Nitinol).
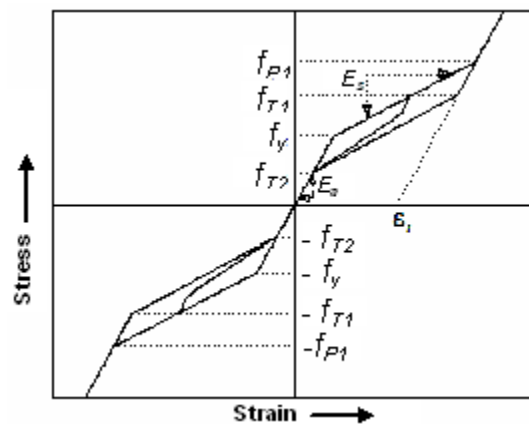

Figure 1 - 1D-superelastic model of SMA incorporated in FE Pacakges[15].

Since most civil engineering applications of SMA are related to the use of bars and wires, one-dimensional phenomenological models are often considered suitable. Several researchers have proposed uniaxial phenomenological models for SMA[10, 11]. The superelastic behavior of SMA has been incorporated in a number of finite element packages, e.g. ANSYS 10.0[12], ABAQUS 6.4[13] and Seismostruct 4.0.2[14] where the material models have been defined using the models of Auricchio et al.[15], Auricchio and Taylor[16], and Auricchio and Sacco[17], respectively. Figure 1 shows the 1D-superelastic model used in ANSYS 10.0[12] where SMA has been subjected to multiple stress cycles at a constant temperature and undergoes stress induced austenite-martensite transformation. The parameters used to define the material model (Figure 1)

are f_y (point C); f_{P1} (point E); f_{T1} (point F); f_{T2} (point G); superelastic plateau strain length, ε_l; moduli of elasticity, E_s and E_a; and the ratio of f_y under tension and compression, α.

Experimental study on SMA RC elements
This section briefly describes the available experimental studies conducted on SMA RC beam-column elements under seismic loading

A large-scale beam-column joint was tested under reversed cyclic loading by Youssef et al.[8]. The joint was reinforced with SMA at the plastic hinge region of the beam, along with regular steel in the remaining portion of the joint (specimen JBC-2). The joint was designed according to Canadian standards[18]. The detailed design of JBC-2 is given in Figure 2 where single barrel screw lock couplers[19] were used for connecting steel and SMA rebars. The couplers used are mechanical connectors consisting of smooth shaped steel sleeves with converging sides. Each end of the reinforcing bars is inserted into one of the coupler ends until it reaches the middle pin (center stop). Both rebars meet head to head separated by a pin at the middle. Screws with smooth ends are used to hold the rebars, which are tightened until their heads are sheared off indicating that the required torque is reached. The material properties for JBC-2 are presented in Table 1.
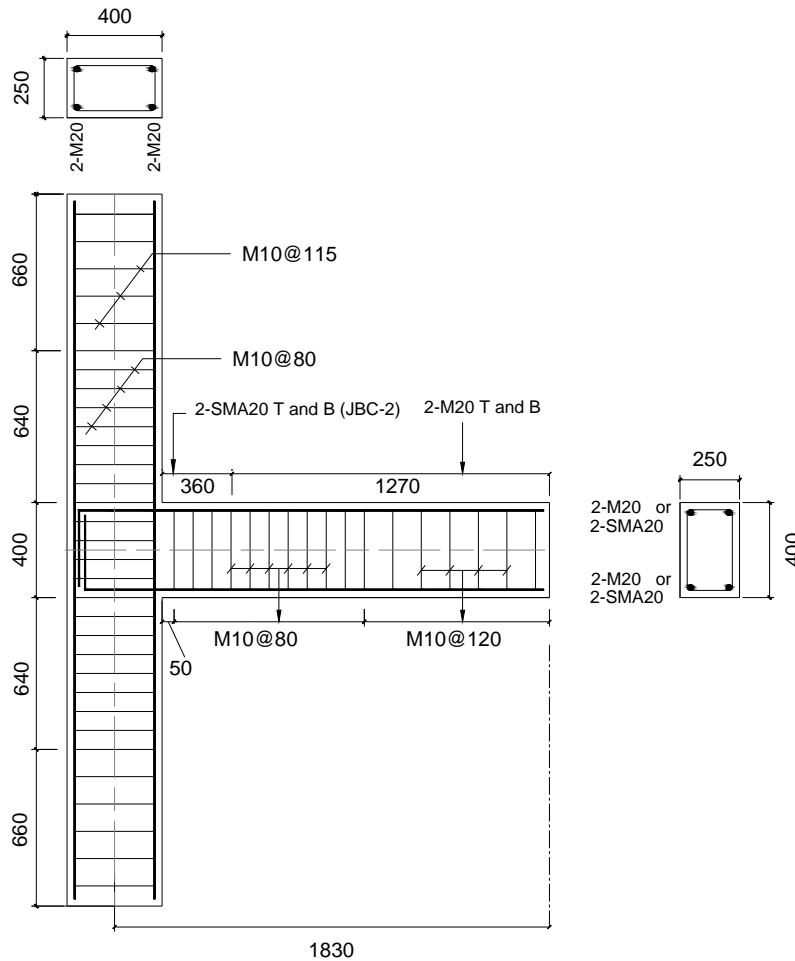

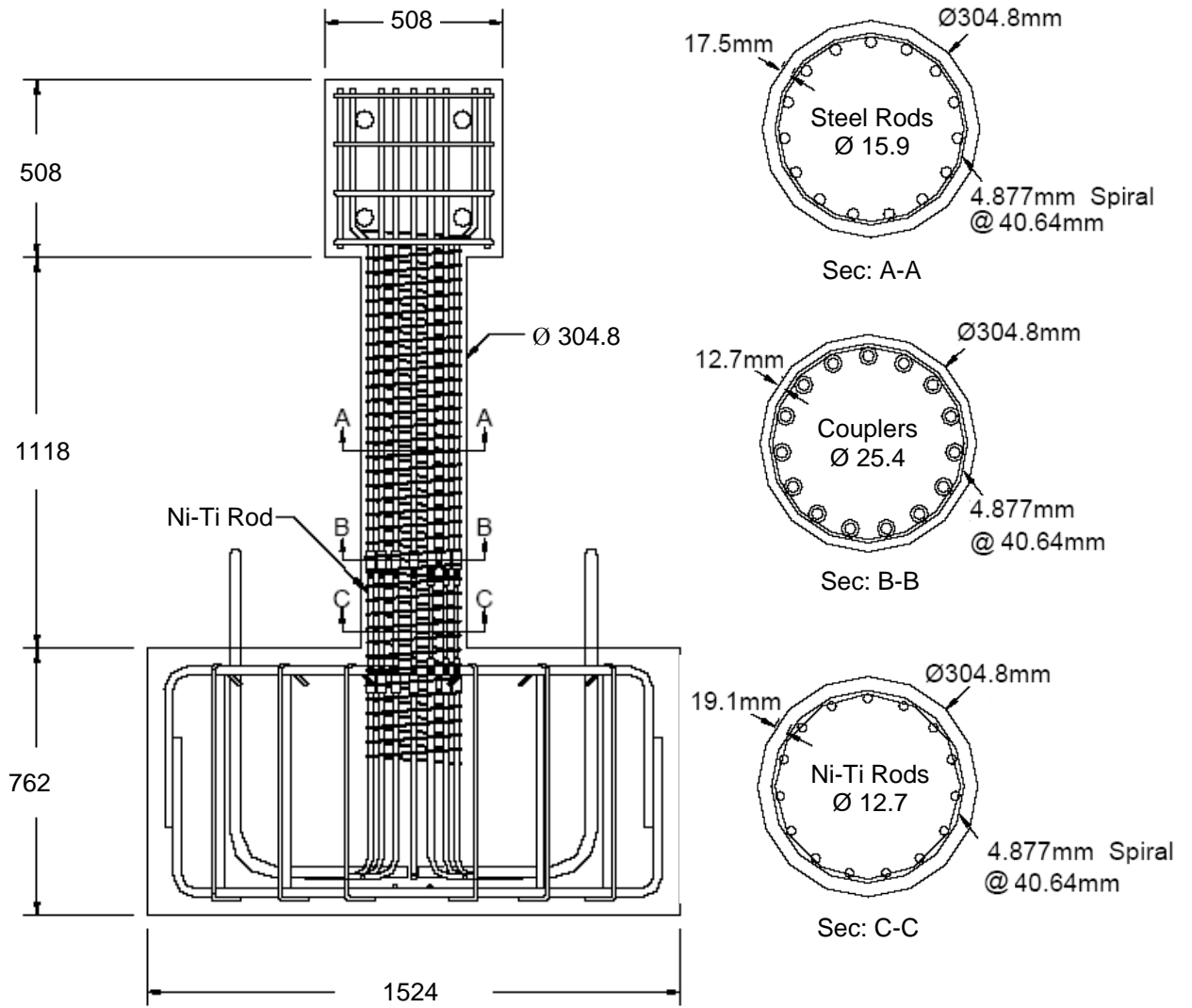**Figure 2 - Reinforcement details of specimen JBC-2 (all dimensions in mm, 25.4 mm = 1 in).**

Figure 3 - Reinforcement details of SMA RC Column[7] (25.4 mm = 1 in).

Table 1: Material properties for specimens JBC-2 and SMAC-1, (6.895 MPa = 1 ksi)

Material	Property	JBC-2[8]	SMAC-1[7]
Concrete	Compressive strength (MPa)	53.7	43.8
	Strain at peak stress (%)	0.2	0.2
	Tensile strength (MPa)	2.8	4.0
Longitudinal steel (JBC-2: Ø19.5 mm, SMAC-1:Ø15.9mm)	Yield strength (MPa)	450	439
	Ultimate strength (MPa)	650	708
	Young's modulus (GPa)	193	200
Transverse steel (JBC-2: Ø11.3 mm, SMAC-1: Ø4.9 mm)	Yield strength (MPa)	422	469
	Ultimate strength (MPa)	682	540
SE SMA (JBC-2: Ø20.6 mm, SMAC-1:Ø12.7mm)	Modulus of elasticity, E_{SMA} (GPa)	62.5	39.7
	f_y as in Figure 1 (MPa)	401	379
	f_{P1} as in Figure 1 (MPa)	510	405
	f_{T1} as in Figure 1 (MPa)	370	180
	f_{T2} as in Figure 1 (MPa)	130	100
	ε_l as in Figure 1 (%)	6.00	5.5

Two quarter-scale spiral RC columns representing RC bridge piers were designed, constructed and tested using a shake table by Wang[7]. Figure 3 shows the reinforcement detailing of the bridge pier (specimen SMAC-1) where SMA rebars are placed at the plastic hinge region and connected to the steel rebars with threaded mechanical couplers. The mechanical properties of the materials used are presented in Table 1. It was observed that SMA-RC columns were superior to conventional steel-RC columns in limiting relative column top displacement and overall residual displacements; they withstood larger earthquake amplitudes compared to that for conventional columns.

Finite element modelling

In the present section, several inelastic time-history analyses have been performed to predict the performance of steel and SMA RC structural elements using a FE program and compare the results with corresponding experimental data. The fibre modelling approach has been employed to represent the distribution of material nonlinearity along the length and cross-sectional area of the member. 3D beam-column elements have been used for modelling the beam and column where the sectional stress-strain state of the elements is obtained through the integration of the nonlinear uniaxial stress-strain response of the individual fibres in which the section has been subdivided following the spread of material inelasticity within the member cross-section and along the member length. Concrete and steel have been modelled using models of Martinez-Rueda and Elnashai[20] and Monti and Nuti[21], respectively. SMA has been modelled according to the model of Auricchio and Sacco as discussed earlier. Figure 1 shows the 1D-superelastic model used in the FE program where SMA has been subjected to multiple stress cycles at a constant temperature and undergoes stress induced transformations. The parameters used to define the material model are: 1) yield stress, f_y; 2) maximum stress up to the superelastic strain range, f_{P1}; 3) first stage of unloading stress, f_{T1}; 4) second stage of unloading stress, f_{T2}; 5) superelastic plateau strain length, ε_l, and 6) modulus of elasticity, E (Table 1).

Finite element analysis: SMA RC beam-column joint

This section describes FE analyses carried out to validate the results of the FE program with experimental data. The load-displacement relationship has been used for this purpose.

A FE mesh has been developed for the beam-column joint specimen JBC-2 where the geometry and material properties were taken from the experimental data provided by Youssef et al.[8]. Figure 4(a) presents the experimental results of the tested specimen showing the beam tip load versus beam tip displacement. Figure 4(b) illustrates the numerical results predicted by the FE analysis. The ultimate beam tip load was predicted as 62.7 kN (14.1 kip) at a tip displacement of 72 mm (2.83 in) compared to the experimental result of 68.1 kN (15.3 kip) at the same tip displacement. The total predicted energy dissipation was 19.7 kN.m (14.54 kip.ft), which is 17% higher than that of the experimental value. Besides the variation in initial stiffness of the predicted load-displacement relationship compared to that of the experimental results, the numerical model was capable of predicting the force-displacement behaviour of the SMA RC joint with reasonable accuracy. The disparity in the initial stiffness might be due to slippage of the smooth SMA rebars in the joint region of the tested specimen. The predicted results using the FE technique can be refined by introducing proper bond-slip model at the joint region as described earlier. The bond-slip relationship can also be incorporated at the joint region of the FE model by applying a rotational spring simulating the slippage of SMA rebar.
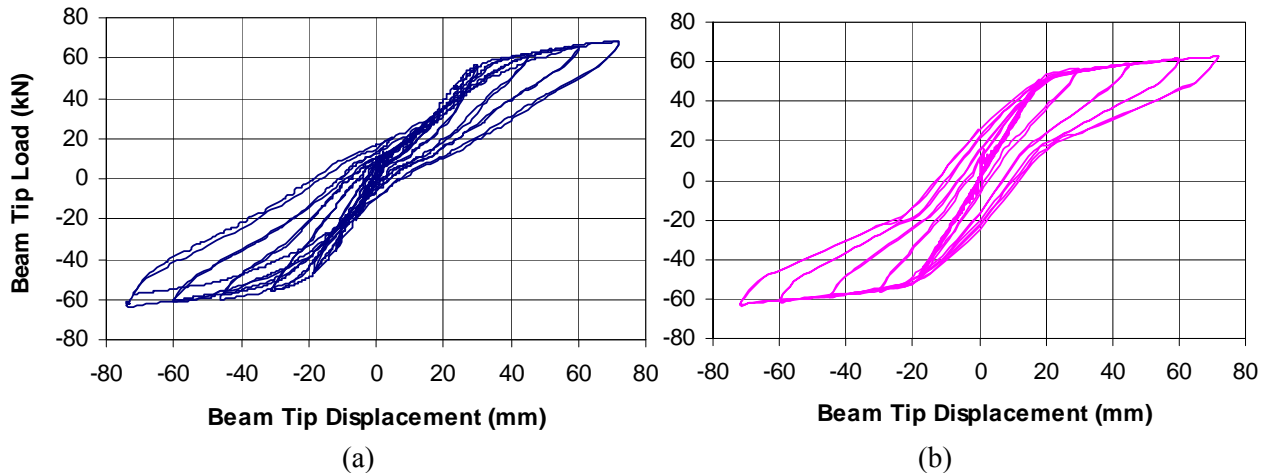
Figure 4 - Beam tip load versus tip-displacement of JBC-2: (a) experimental results[8], and (b) analytical results (4.448 kN = 1 kip, 25.4 mm = 1 in).
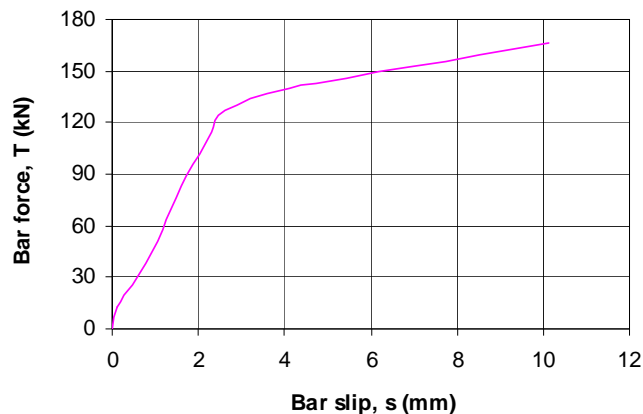

Figure 5 - Resultant bar slip, s inside the coupler with respect to bar force, T(4.448 kN = 1 kip, 25.4 mm = 1 in).

An experimental investigation was carried out to determine the slippage of SMA rebars through couplers by a simple pullout test. Steel and SMA rebars were inserted at each end of the coupler, the screw heads were sheared off by applying prescribed torques. Then the coupler arrangement was tested using a universal testing machine under tension only. An extensometer was clamped to the steel and SMA rebars to determine the change in length. The slippage, s inside the coupler was then calculated by subtracting the axial elongation of steel (s_{st}) and SMA (s_{SMA}) rebars due to tensile forces from the extensometer reading, s_e. Figure 5 illustrates the bar force versus slippage of SMA rebar in the coupler. This figure was then used to construct the moment-rotation relationship due to slippage. From numerical analysis, the bar force, T is calculated for a corresponding beam tip load, P (Figure 6(a)).
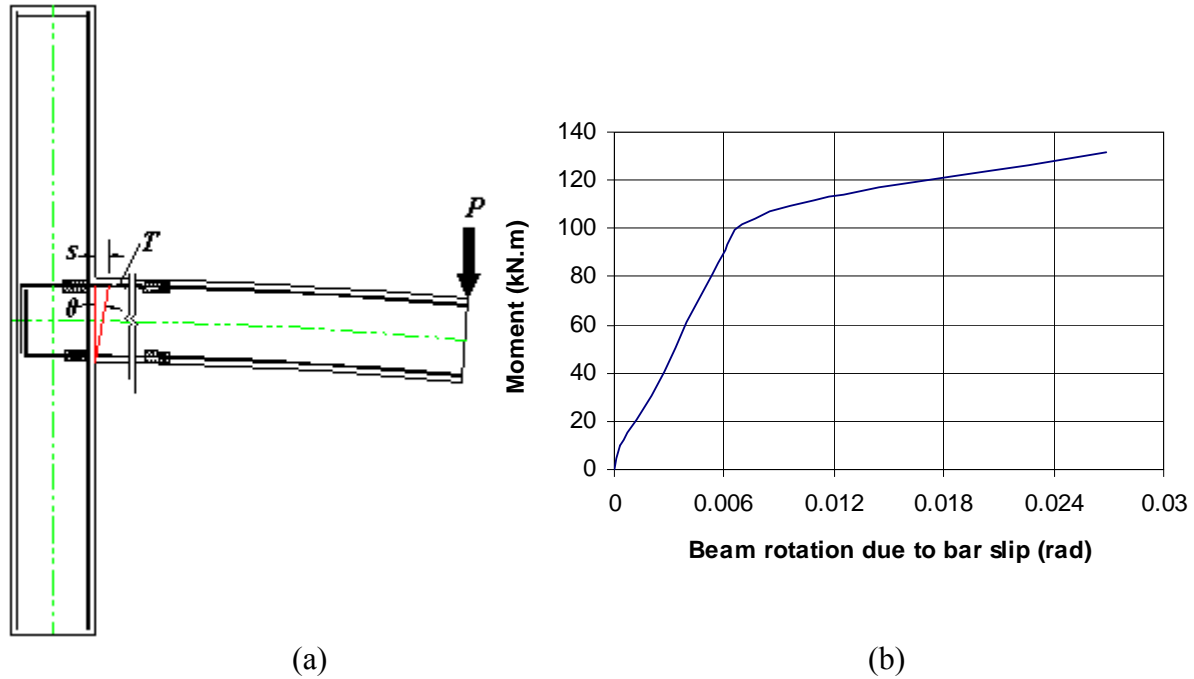
(a)   (b)

Figure 6 - (a) SMA bar slip at joint due to beam tip load, and (b) moment-rotation relationship due to bar slip.

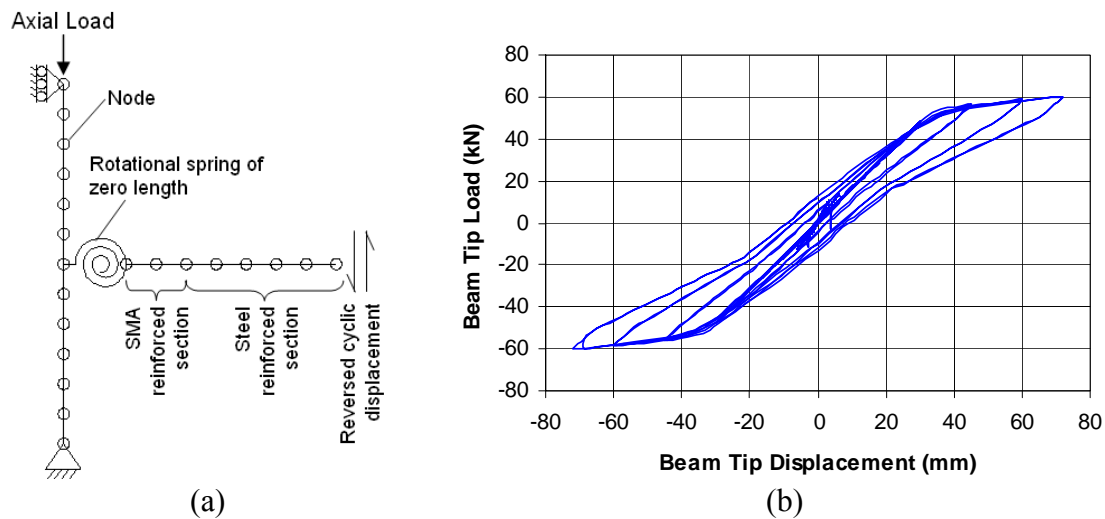(a)   (b)

Figure 7 - (a) FE model of a SMA-RC exterior joint, where bond-slip is incorporated by a rotational spring, and (b) beam tip load-displacement relationship of JBC-2 with bond slip model (4.448 kN = 1 kip, 25.4 mm = 1 in).

Using the relationship of Fig. 5 the slip at the joint, s is obtained, which allows calculating beam rotation, $\theta = s/(h-d')$ due to bar slip, where, h is the beam depth and d' is the distance from the centre of the top bar to the top beam face. After calculating θ, the corresponding moment is calculated by multiplying the moment arm with P. Repeating the same procedure, the moment-rotation relationship is established as shown in Figure 7(b). This relationship has been used for the analytical model of JBC-2, which has been represented by a rotational spring at its joint.

The adapted FE model is presented in Fig. 7(a). The numerical results predicted by the new model show good agreement with the experimental results varying by 11% for beam tip load under an equal amount of tip displacement as shown in Fig. 7(b). The predicted initial stiffness was similar to the experimental result. The cumulative energy dissipation was found as 16.7 kN.m (12.34 kip.ft) from the load-displacement curve of the test result, whereas the amount of energy dissipation obtained from the predicted result was 14.0 kN.m (10.33 kip.ft), which is 16.2% lower than the experimental result.

Finite element analysis: SMA RC Column

Two quarter-scale spiral RC columns representing RC bridge piers were designed, constructed and tested using a shake table by Wang[7]. SMA rebars were placed at the plastic hinge region and connected to the steel rebars with mechanical threaded couplers. An inelastic dynamic analysis has been performed to predict the performance of the bridge pier tested by Wang[7]. SMA has been modelled according to Fig. 2. A finite element model for the bridge pier is shown in Fig. 8(a). Here no special modelling technique has been incorporated for bar couplers since experimental results showed full capacity for transferring forces from SMA to steel rebar with negligible slippage. The pier was subjected to a series of scaled motions ranging from 15% to 300% of the base acceleration time history as shown in Fig. 8(b).
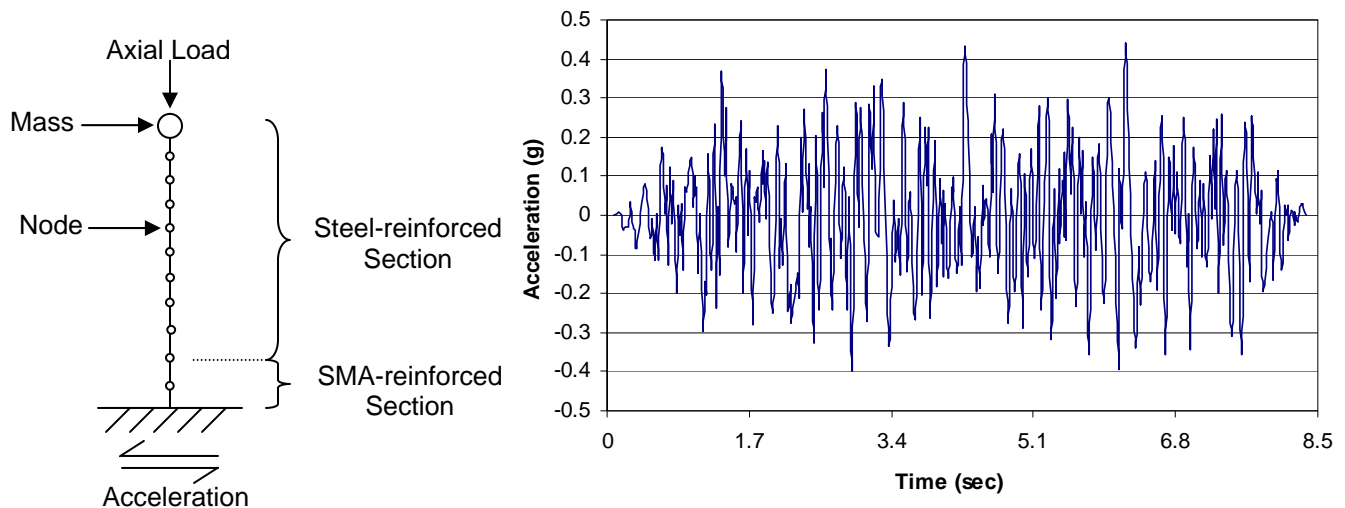

Figure 8 - (a) FE model of a SMA-RC column, and (b) base acceleration time-history applied in SMA-RC column[7].

Figure 9(a) shows the performance of the bridge pier under shake table testing. Figure 9(b) depicts the predicted base shear-tip displacement of the numerical model which seems to be fairly accurate as compared to the experimental results of Wang[7]. The maximum base shear and the tip displacement were predicted as 81.5 kN and 62.0 mm compared to experimental values of 77.2 kN and 66.0 mm, respectively. The numerical results predicted by the FE model show good agreement with corresponding experimental results varying only by 5.6% for the base shear and 6.1% for the tip displacement. The cumulative energy dissipation was calculated as 48.2 kN.m from the predicted load-displacement curve, whereas the amount of energy dissipation obtained from the experimental result was 44.0 kN.m, which is only 9.4% lower than the calculated result. The SMA-RC column failed by concrete crushing and yielding of SMA rebar within the

superelastic strain range and the displacement ductility was measured as 5.9, whereas in the numerical analysis, the model also failed due to crushing of concrete and yielding of SMA within superelastic strain limit with a displacement ductility of 6.7.
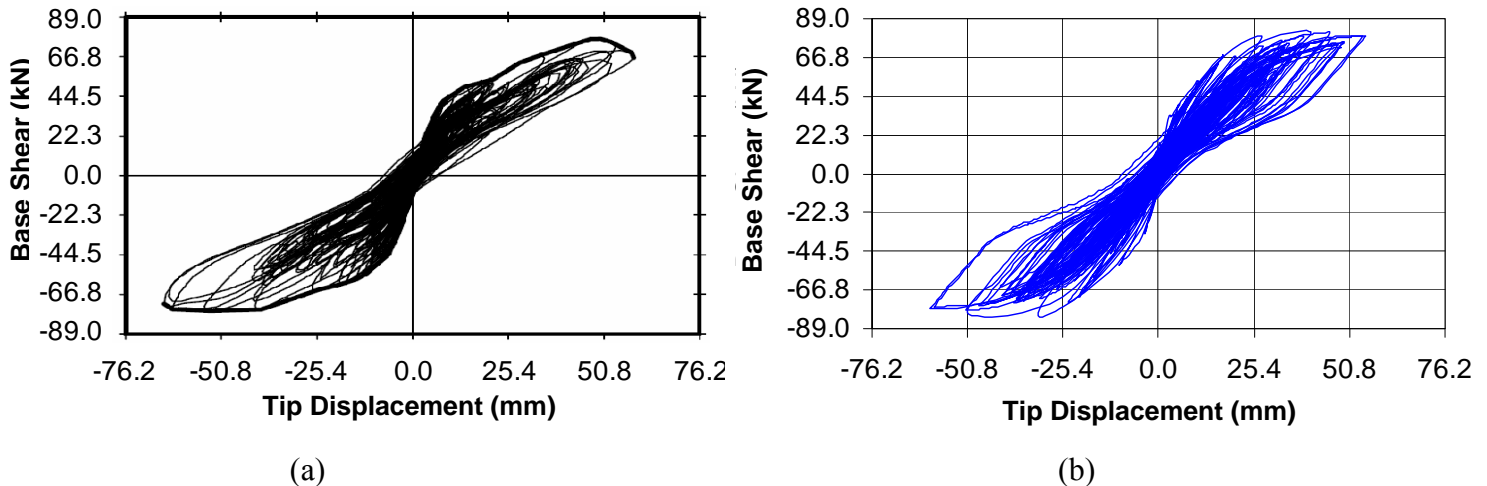

(a)   (b)

Figure 9 - Base shear versus tip-displacement for SMA-RC bridge pier: (a) experimental results[7], and (b) analytical results.

Conclusions
This paper examines the seismic behaviour of SMA RC beam-column elements using numerical tools. The objective of this study is to make analytical prediction of the behaviour of SMA-RC beam-column elements in terms of load-displacement relationship and compare them with their corresponding experimental results.

Both specimens JBC-2 and SMAC-1 have been analyzed under cyclic displacement loading with the use of a FE program and their performances have been compared with corresponding experimental results. The numerical results indicate that the FE program can predict the load-displacement curve with reasonable accuracy. Barlock type couplers may cause higher slippage compared to that of threaded couplers, therefore, an adequate bond-slip model should be incorporated for an accurate prediction of the load-displacement relationship while using barlock type couplers.

References
1. Alam, M.S., Youssef, M.A., and Nehdi, M., 2007, Utilizing shape memory alloys to enhance the performance and safety of civil infrastructure: a review. Canadian Journal of Civil Engineering, 34, 1075-1086.
2. Tamai, H., Miura, K., Kitagawa, Y., and Fukuta, T., 2003, Application of SMA rod to exposed-type column base in smart structural system, the Proc. of SPIE, 5057, 169-177.
3. Dolce, M., Cardone, D., Marnetto, R., Mucciarelli, M., Nigro, D., Ponzo, F.C., and Santarsiero, G., 2004, Experimental static and dynamic response of a real RC frame upgraded with SMA re-centering and dissipating braces, the Proc. of the 13th World Conf. on Earthquake Engg., Canada, 2004; Paper no. 2878.
4. Maji, A.K., and Negret, I., 1998, Smart prestressing with shape memory alloy. Journal of Engineering Mechanics 1998, 124, 1121-1128.

5. Clark, P.W., Aiken, I.D., Kelly, J.M., Higashino, M., and Krumme, R., 1995, Experimental and analytical studies of shape-memory alloy dampers for structural control, the Proc. of SPIE 1995; 2445, 241-251.
6. Andrawes, B., and Desroches, R., 2005, Unseating prevention for multiple frame bridges using superelastic devices, Smart Materials and Structures 2005, 14, S60-S67.
7. Wang, H., 2004, A study of RC columns with shape memory alloy and engineered cementitious composites, M.Sc. Thesis, Department of Civil Engineering, University of Nevada, Reno.
8. Youssef, M.A., Alam, M.S., Nehdi, M., 2007, Experimental investigation on the seismic behaviour of beam-column joints reinforced with superelastic shape memory alloys, Journal of Earthquake Engineering, accepted November, 2007.
9. Wilson, J.C., and Wesolowsky, M.J., 2005, Shape memory alloys for seismic response modification: a state-of-the-art review, Earthquake Spectra 2005; 21, 569-601.
10. Tanaka, K., and Nagaki, S., 1982, Thermomechanical desription of materials with internal variables in the process of phase transitions, Ingenieur-Archiv 1982, 51, 287-299.
11. Auricchio, F., and Lubliner, J., 1997, Uniaxial model for shape-memory alloys, International Journal of Solids and Structures, 34, 3601-3618.
12. ANSYS, Inc. Version 10.0. South Pointe, Canonsburg, PA, USA, 2005.
13. Hibbitt, Karlsson and Sorensen. Abaqus User's Manual, Version 6.4, Pawtucket, RI, 2003.
14. SeismoStruct Help file 2007, Version 4.0.2 accessed on Feb 2007, available at http://www.seismosoft.com/SeismoStruct/index.htm.
15. Auricchio, F., Taylor, R.L., and Lubliner, J., 1997, Shape-memory alloys: macromodelling and numerical simulations of the superelastic behaviour, Computer Methods in Applied Mechanics and Engineering, 146, 281-312.
16. Auricchio, F., and Taylor, R.L., 1996, Shape memory alloy superelastic behavior: 3D finite-element simulations, the Proc. of SPIE, 2779, 487-492.
17. Auricchio, F., and Sacco, E., 1997, Superelastic shape-memory-alloy beam model, Journal of Intelligent Material Systems and Structures, 8, 489-501.
18. Design of Concrete Structures, CSA A23.3-04, Canadian Standards Association, Rexdale, Ontario, Canada, 2004, 240 pages.
19. Barsplice Products Inc, Zap Screwlok ® Mechanical splices and connectors for reinforcing bars, April 2006, http://www.barsplice.com/BPI_Scans/Zap_Data-Sheet_RevA.pdf.
20. Martinez-Rueda, J.E., and Elnashai, A.S., 1997, Confined concrete model under cyclic load, Materials and Structures, 30, 139-147.
21. Monti, G., and Nuti, C., 1992, Nonlinear cyclic behaviour of reinforcing bars including buckling. Journal of Structural Engineering, ASCE, 118, 3268-3284.